

Influence of misfit dislocations on thermal quenching of luminescence in $\text{In}_x\text{Ga}_{1-x}\text{As}/\text{GaAs}$ multiple quantum wells

K. Rammohan, H. T. Lin, and D. H. Rich^{a)}

Photonic Materials and Devices Laboratory, Department of Materials Science and Engineering, University of Southern California, Los Angeles, California 90089-0241

A. Larsson

Department of Optoelectronics and Electrical Measurements, Chalmers University of Technology, Göteborg, Sweden

(Received 7 June 1995; accepted for publication 24 August 1995)

The temperature dependence of the cathodoluminescence (CL) originating from $\text{In}_{0.21}\text{Ga}_{0.79}\text{As}/\text{GaAs}$ multiple quantum wells has been studied between 86 and 250 K. The CL intensity exhibits an Arrhenius-type dependence on temperature (T), characterized by two different activation energies. The influence of misfit dislocations and point defects associated with strain relaxation on the thermal quenching of luminescence has been investigated, and the spatial variation in the activation energies has been examined. The CL intensity dependence on temperature for $T \leq 150$ K is controlled by thermally activated nonradiative recombination. For $T \geq 150$ K the decrease in CL intensity is largely influenced by thermal re-emission of carriers out of the quantum wells. © 1995 American Institute of Physics.

I. INTRODUCTION

Strained-layer quantum wells (QWs) of $\text{In}_x\text{Ga}_{1-x}\text{As}$ grown epitaxially on GaAs have attracted considerable attention because of their promise for novel photonic device applications.¹⁻⁴ Such devices may require operation under various electron-hole excitation densities and temperature. The presence of strain-induced defects will introduce nonradiative recombination centers whose influence on the optical properties will be temperature and excitation dependent. Hence, it is essential to study the luminescence efficiency of quantum well structures as a function of temperature in an attempt to better understand the interplay between thermal activation of excess carriers and defect-induced recombination.

Some previous work has focused on the investigation of misfit dislocations and the associated dark line defects (DLDs) with spatially resolved experiments like scanning cathodoluminescence (CL), transmission electron microscopy (TEM), and a combination of both methods.⁵⁻⁷ While the temperature dependence of luminescence in quantum wells and superlattices has been investigated previously,^{8,9} little work that addresses the effects of thermal quenching of luminescence by misfit dislocations has been reported. Thermal quenching of the luminescence in QWs has been interpreted in several ways by different authors, and has been attributed to thermal dissociation of excitons and thermally activated nonradiative recombination,¹⁰ or due to thermal emission of carriers out of the QWs, resulting in a reduction of luminescence intensity at higher temperatures.¹¹

In this work, we examine the influence of misfit dislocations and point defects associated with strain relaxation on the thermal quenching of luminescence. The activation energies associated with the thermal quenching of luminescence

vary spatially in close proximity to defects, and we have utilized a new approach which uses spatially resolved CL to image these activation energies.

II. EXPERIMENT

Multiple-quantum-well (MQW) samples were grown by molecular beam epitaxy using standard In, Ga, and As solid sources. The samples designated D38 and D18 consist of 44 periods of 65 Å $\text{In}_{0.21}\text{Ga}_{0.79}\text{As}$ MQWs with barrier thicknesses of 115 and 400 Å, respectively. In sample D179, a 65 Å MQW structure having 100 and 1230 Å barriers with 14 periods (28 QWs) were grown. The samples were investigated with scanning CL microscopy. CL measurements were performed with a JEOL 840-A thermionic emission scanning electron microscope. A liquid-nitrogen-cooled Ge p - i - n detector was used to measure the luminescence dispersed by a 0.25 m monochromator. An electron beam current of ~ 7 nA and beam energy of 20 keV were used to probe the samples. CL spectra and images were recorded for various different temperatures between 86 and 250 K.

III. RESULTS AND DISCUSSION

The temperature dependence of the electron-to-heavy-hole excitonic luminescence intensity for sample D18 is shown in Fig. 1 for temperatures between 86 and 250 K. The data labeled A correspond to the integrated CL spectral intensity, I_{MQW} , measured while the electron beam was scanning a $128 \mu\text{m} \times 94 \mu\text{m}$ region. The CL intensity reduced by about two orders of magnitude as the temperature increased from 86 to 250 K. From Fig. 1, it is evident that there exists two temperature ranges which show an Arrhenius behavior. This behavior indicates the presence of two different thermally activated processes responsible for the reduction in

^{a)} Author to whom correspondence should be addressed; Electronic mail: danrich@usc.edu

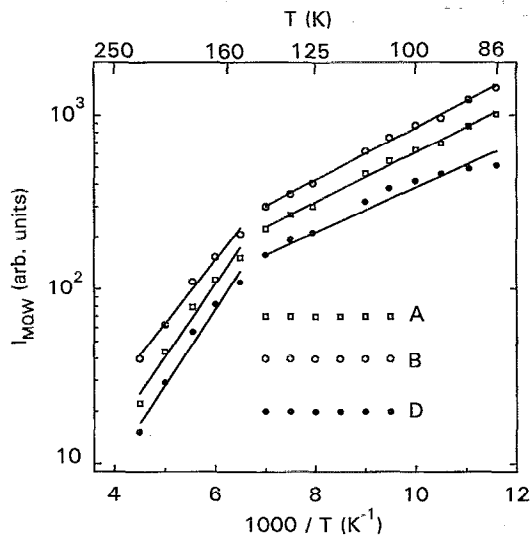


FIG. 1. Temperature dependence of CL intensity for sample D18. The data labeled A corresponds to the integrated CL spectral intensity, I_{MQW} , measured while the electron beam was scanning a $128 \mu\text{m} \times 94 \mu\text{m}$ region. The data labeled B and D correspond to the intensity obtained from bright and dark regions, respectively, shown in Fig. 2(a). The solid lines are linear fits to the data.

luminescence efficiency. The activation energies for both cases are obtained from the straight line portions of the $\log I_{MQW}$ vs $1/T$ plots; activation energies of ~ 27 and ~ 79 meV are obtained in the temperature ranges of 86–150 K and 150–250 K, respectively.

In order to study local variations in the activation energy we performed CL imaging of the MQW excitonic luminescence at various different temperatures between 86 and 250 K. A scanning area of $128 \mu\text{m} \times 94 \mu\text{m}$ was discretized into 640×480 pixels. CL studies enable a mapping of local changes in activation energies on the scale of $\sim 1 \mu\text{m}$ in GaAs, as the resolution is limited by the minority-carrier diffusion and the size of the peak-shaped excitation volume. The activation energy (E_a) was determined at all spatial (x, y) positions; gray-scale images representing the activation energies are shown in Fig. 2. In order to determine E_a at each pixel position, 14 images were obtained for various fixed temperatures between 86 and 250 K. The slopes were determined separately for the two temperature ranges observed in Fig. 1 using a least-squares fitting at each (x, y) position.

The monochromatic CL images obtained at 86 K for samples D18, D38, and D179 are shown in Figs. 2(a), 2(b), and 2(c), respectively. Figures 2(d), 2(e), and 2(f) represent a spatial mapping of the activation energies for the same regions shown in Figs. 2(a), 2(b), and 2(c), respectively, for the intermediate temperature range (86–150 K). Figures 2(g), 2(h), and 2(i) represent a spatial mapping of the activation energies obtained in the high-temperature range (150–250 K). The mapping of E_a into a gray-scale representation is shown by the gray bar indicating the activation energy scale. Plots of $\log I_{MQW}$ vs $1/T$ for sample D18 are shown in Fig. 1 for two arbitrary local regions, labeled B and D (for bright and dark regions). Long streaks of constant gray shade are

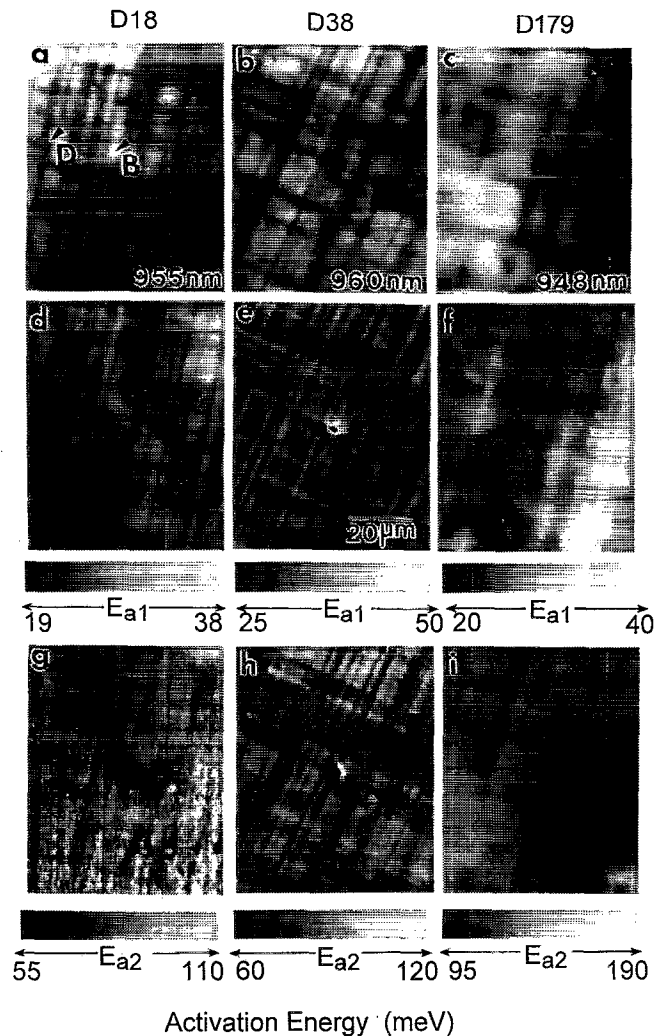


FIG. 2. Monochromatic CL images (at $T=86$ K) obtained at 955, 960, and 948 nm for samples D18, D38, and D179 are shown in (a), (b), and (c), respectively. The activation energy images of E_{a1} obtained in the intermediate temperature range (86–150 K) for the same regions shown in (a), (b), and (c) are shown in (d), (e), and (f), respectively. The activation energy images of E_{a2} obtained in the high-temperature range (150–250 K) is shown in (g), (h), and (i), respectively. A scale showing the mapping of the activation energies is shown below each image. The length scale for all images is shown in (e).

seen to run along the high symmetry $\langle 110 \rangle$ directions in Fig. 2 in both the monochromatic and activation energy CL images. In monochromatic CL imaging, dislocations appear as dark line defects (DLDs) as a result of a localized reduction of luminescence efficiency due to an enhanced nonradiative recombination.⁵ Comparing Figs. 2(a) and 2(d), we observe that regions containing misfit dislocations (dark regions) show a lower activation energy than regions absent of DLDs [bright regions in Fig. 2(a)]. However, in the high-temperature range [Fig. 2(g)], there is a reversal of contrast as compared to Fig. 2(a), i.e., the bright regions in Fig. 2(a) exhibit a lower activation energy while the dark regions (DLDs) exhibit a higher activation energy. In order to further illustrate the spatial correlation existing between sets of images for a given sample, we show stack plots for sample D38 in Fig. 3, corresponding to images in Figs. 2(b), 2(e), and

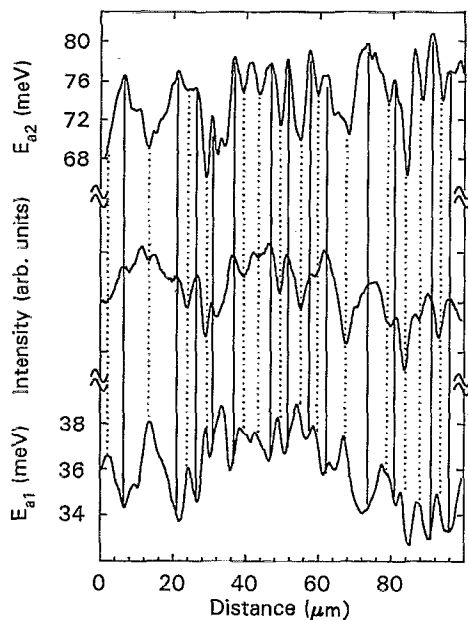


FIG. 3. Stack plot of CL intensity, activation energies E_{a1} and E_{a2} for an arbitrary line scan done along the $\langle 110 \rangle$ direction for sample D38. The spatial correlation of regions showing decreased luminescence efficiency, higher E_{a1} , and lower E_{a2} (indicated by dotted lines) and increased luminescence efficiency, lower E_{a1} , and higher E_{a2} (indicated by solid lines) is observed.

2(h). The luminescence intensity, and the activation energies for the intermediate (E_{a1}) and high-temperature range (E_{a2}) are plotted as a function of the distance taken along an arbitrary $\langle 110 \rangle$ -oriented line.

The activation energy E_{a1} ranges from ~ 23 to 38 meV for all three samples. Prior to the capture of electrons and holes into the QWs, free carriers which have thermalized down to the band edges must diffuse along the GaAs barriers. A recent study showed that the activation energy for ambipolar diffusive transport, E_D , in a nipi-doped $\text{In}_{0.2}\text{Ga}_{0.8}\text{As}/\text{GaAs}$ MQW structure possessing similar barrier and QW thicknesses has a lower limit of ~ 29 meV.¹² It is plausible that the same defects which impede ambipolar diffusion also serve as nonradiative recombination centers. Thus, once sufficient thermal energy is attained to surmount the defect-induced barriers, the mobile carriers also become more susceptible to nonradiative recombination at these same centers before capture in the QWs, thereby explaining the similar values of E_{a1} and E_D . Likewise, it is also possible that ionization of free and bound excitons in the QWs, prior to radiative recombination, also contributes to the decrease in I_{MQW} in the intermediate temperature range since defects in the QWs should also exhibit similar thermal barriers. The binding energy of the exciton is ~ 7 meV, requiring additional thermal activation over defect-induced barriers in the QWs prior to nonradiative recombination.

For the intermediate temperature range (86–150 K), the bright regions in samples D179 and D38 exhibit a smaller activation energy E_{a1} than that of dark regions (DLDs) while the bright regions in sample D18 exhibit a larger activation energy than the dark regions. Consistent with the above de-

TABLE I. The effective barrier heights, E_{BC} and E_{BV} for re-emission out of the quantum well. These heights are calculated as $E_{\text{BC}} = \Delta E_C - E_{e1}$ and $E_{\text{BV}} = \Delta E_V - E_{hh1}$, where ΔE_C and ΔE_V are the conduction- and valence-band offsets between $\text{In}_{0.21}\text{Ga}_{0.79}\text{As}$ and GaAs, and E_{e1} and E_{hh1} denote the calculated first electron and heavy-hole subband energy.

	E_{BC} (meV)	E_{BV} (meV)
Fully strained	111	58
Fully relaxed	159	80

scription, we expect that diffusing carriers in the GaAs barriers of dark regions will experience an enhanced probability for nonradiative recombination prior to their capture in the InGaAs QWs. The bright regions which contain a reduced density of defects (i.e., density of misfit dislocations and point defects) in all three samples exhibit similar activation energies (26–33 meV). The decrease [as shown in Fig. 2(d)] or the increase [as shown in Figs. 2(e) and 2(f)] in activation energy of the dark regions as compared to the bright regions is evidently due to a change in the distribution of defects (both in density and type) in the dark regions caused by the differences in the GaAs barrier thickness between samples. Prior studies by Hillmer *et al.*¹³ have shown that the 2D carrier mobilities remain nearly constant between 80 and 150 K and 2D carrier diffusivity increases by a factor of less than 2 between 80 and 150 K. The excitation volume of a 20 keV electron beam limits the spatial resolution to ~ 1.5 μm in GaAs.¹⁴ Thus, small changes in carrier diffusion length with temperature will negligibly affect the local changes in activation energy that are observed here.

The activation energy E_{a2} is most likely a result of re-emission of carriers which have been captured in the QWs since E_{a2} varies from ~ 65 to ~ 130 meV, for all three samples, and is close to the electron and hole barrier heights (ground state to unbound states) for $\text{In}_{0.2}\text{Ga}_{0.8}\text{As}/\text{GaAs}$ MQWs.¹⁵ A similar re-emission of captured carriers has previously been observed in AlGaAs/GaAs MQW systems.¹¹ For a region which contains misfit dislocations, the local reduction in strain results in a lowering of the band gap and an increase in the effective barrier height for electrons (E_{BC}) and holes (E_{BV}) as compared to the effective barrier height for electrons and holes in a bright region exhibiting a larger local strain. It is possible that the enhanced activation energy exhibited by the DLDs in Figs. 2(a) and 2(c) is due to the larger barrier heights for carrier re-emission exhibited in the partially relaxed regions. The limiting cases for the QW barrier heights are shown in Table I, as calculated with a standard transfer matrix method.¹⁵ The barrier heights for the partially relaxed regions will be intermediate to the fully strained and relaxed cases. In the high-temperature range (150–250 K), the barrier regions exhibit a lower activation energy than the dark regions in samples D18 and D179, which is consistent with the lower effective barrier height for electrons and holes listed in Table I in a quantum well subject to a larger strain. The converse is true for D38, which exhibits a higher activation energy near bright regions (away from DLDs). The nonradiative recombination that gives rise

to DLDs is a result of recombination at cores of misfit dislocation and point defects in the vicinity of the dislocations.⁵ It is possible that D38, which has the smallest average GaAs barrier layer thickness of all the samples, may contain the largest average point defect density. This enhanced defect density could act to reduce the activation energy for nonradiative recombination near the DLDs, in competition with the opposite tendency of a higher activation barrier caused by a greater strain relaxation. Thus, the behavior of the activation energies near DLDs reflects the extent to which both (i) strain relaxation and (ii) defect centers will influence the thermal re-emission of carriers from the QWs.

IV. CONCLUSION

In summary, we have studied the temperature dependence of CL intensity from $\text{In}_{0.21}\text{Ga}_{0.79}\text{As}/\text{GaAs}$ multiple quantum wells. Using a new CL imaging analysis, we have observed local variations in the activation energies which are likely caused by local fluctuations in the band edge near misfit dislocations and point defects. A pronounced decrease in CL intensity occurs in both bright and dark regions above 150 K. The magnitude of activation energies observed for the temperatures greater than 150 K indicates that this decrease is probably due to the thermal re-emission of electrons and holes from the quantum wells.

ACKNOWLEDGMENT

This work was supported by the NSF (RIA-ECS) and ARO.

- ¹J. J. Rosenberg, M. Benlamri, P. D. Kirchner, J. M. Woodall, and G. D. Petit, *IEEE Electron. Device Lett.* **EDL-6**, 491 (1985).
- ²G. C. Osburne, *Phys. Rev. B* **27**, 5126 (1983).
- ³G. E. Bir and G. L. Pikus, *Symmetry and Strain Induced Effects in Semiconductors* (Wiley, New York, 1974).
- ⁴J. E. Schirber, I. J. Fritz, and L. R. Dawson, *Appl. Phys. Lett.* **46**, 461 (1985).
- ⁵D. H. Rich, T. George, W. T. Pike, J. Maserjian, F. J. Grunthaner, and A. Larsson, *J. Appl. Phys.* **72**, 5834 (1992).
- ⁶E. A. Fitzgerald, G. D. Ast, P. D. Kirchner, G. D. Petit, and J. M. Woodall, *J. Appl. Phys.* **63**, 693 (1988).
- ⁷K. L. Kavanagh, M. A. Capano, L. W. Hobbs, J. C. Barbour, P. M. J. Marec, W. Schaff, J. W. Mayer, G. D. Petit, J. A. Stroschio, and R. M. Feenstra, *J. Appl. Phys.* **68**, 2739 (1990).
- ⁸D. Bimberg, J. Christen, A. Steckenborn, G. Weimann, and W. Schlapp, *J. Lumin.* **30**, 562 (1985).
- ⁹K. Uno, K. Hirano, S. Noda, and A. Sakaki, *Proceedings of the 19th International Symposium on GaAs and Related Compounds* (IOP, Bristol, 1993), p. 241.
- ¹⁰D. S. Jiang, H. Jung, and K. Ploog, *J. Appl. Phys.* **64**, 1371 (1988).
- ¹¹U. Jahn, J. Menninger, R. Hey, and H. T. Grahn, *Appl. Phys. Lett.* **64**, 2382 (1994).
- ¹²D. H. Rich, K. Rammohan, Y. Tang, H. T. Lin, J. Maserjian, F. J. Grunthaner, A. Larsson, and S. I. Borenstain, *Appl. Phys. Lett.* **64**, 730 (1994).
- ¹³H. Hillmer, A. Forchel, S. Hansmann, M. Morohashi, E. Lopez, H. P. Meier, and K. Ploog, *Phys. Rev. B* **39**, 10901 (1989).
- ¹⁴T. E. Everhart and P. H. Hoff, *J. Appl. Phys.* **42**, 5837 (1971).
- ¹⁵D. H. Rich, H. T. Lin, and A. Larsson, *J. Appl. Phys.* **77**, 6557 (1995).